

# Identification and Validation of a Novel PANoptosis-related Gene Signature for Osteosarcoma as Prognostic Model

Xianglin Peng<sup>1,2</sup> and Wanchun Wang<sup>2</sup>

<sup>1</sup>Department of Orthopaedics, The Second People's Hospital of Huaihua, Huaihua, China

<sup>2</sup>Department of Orthopaedics, The Second Xiangya Hospital of Central South University, Changsha, China

## ABSTRACT

**Objective:** To construct and validate a prognostic model for osteosarcoma prognostication and therapeutic potential of PANoptosis-related genes.

**Study Design:** Observational study.

**Place and Duration of the Study:** Department of Orthopaedics, The Second Xiangya Hospital of Central South University, Changsha, Hunan, China, from August 2021 to January 2024.

**Methodology:** Transcriptomic data from the GEO and TARGET databases were utilised to construct and validate a prognostic model for osteosarcoma. The analysis involved the use of the LASSO Cox-regression method with the *Glmnet* R package to identify key PANoptosis-related genes. Differential gene expression analysis was conducted using the *Limma* R package, and model validation was performed using Kaplan-Meier survival analysis and time-dependent ROC curves.

**Results:** This model, derived from five key PANoptosis-related genes, demonstrated significant predictive capability for patient survival across training and validation cohorts. Further analysis confirmed the model's effectiveness and identified metastasis stage and risk scores as the robust independent prognostic indicators.

**Conclusion:** The prognostic model offers a novel tool for osteosarcoma prognostication and underscores the therapeutic potential of targeting PANoptosis-related pathways.

**Key Words:** PANoptosis-related genes, Osteosarcoma, Prognosis, Bioinformatics, Tumour micro-environment.

**How to cite this article:** Peng X, Wang W. Identification and Validation of a Novel PANoptosis-related Gene Signature for Osteosarcoma as Prognostic Model. *J Coll Physicians Surg Pak* 2024; **34(11)**:1831-1837.

## INTRODUCTION

Osteosarcoma is the predominant malignant tumour of bone, predominantly affecting adolescents and young adults. Globally, osteosarcoma accounts for approximately 3,500 to 4,000 new cases annually, with the highest incidence observed in adolescents and young adults.<sup>1</sup> According to the Global Cancer Observatory (GLOBOCAN) 2020 data, the incidence rates vary geographically, with higher rates reported in regions such as Africa, Asia, and South America.<sup>2</sup> Despite advancement in surgical techniques and adjuvant chemotherapies, the prognosis for patients with metastatic or recurrent osteosarcoma remains dismal.<sup>3,4</sup> The five-year survival rate for these patients has stagnated at around 20% for the past several decades,<sup>5</sup> highlighting an urgent need for the novel prognostic markers and therapeutic targets.

PANoptosis, a term recently coined to describe a form of programmed cell death that involves features of pyroptosis, apoptosis, and necroptosis,<sup>6</sup> has emerged as a crucial mechanism in cancer biology. Contrary to classical pathways of cell demise, PANoptosis is orchestrated by unique triggers, molecular complexes, and executioners.<sup>7</sup> The dysregulation of PANoptosis pathways has been implicated in the initiation, progression, and therapeutic resistance of various cancers, including colon and pancreatic cancer.<sup>8,9</sup>

Recent studies have shed light on the intricate roles of PANoptosis in the context of cancer, offering new insights into tumour biology and potential therapeutic strategies.<sup>10</sup> Recent studies have demonstrated that the recruitment of Receptor-interacting serine / threonine-protein kinase 1 (RIPK1) to secondary signalling complexes, plays a critical role in the resistance of osteosarcoma to TRAIL-based therapies.<sup>11</sup> Ning *et al.*'s work also revealed that osteosarcoma is characterised by the decreased expression of *Caspase-8*, which correlates with increased cell proliferation and reduced apoptosis, suggesting its roles as potential markers and therapeutic targets in osteosarcoma treatment strategies.<sup>12</sup> Thus, understanding the role of PANoptosis-related genes in osteosarcoma could unveil new avenues for prognostication and treatment.

Correspondence to: Dr. Wanchun Wang, Department of Orthopaedics, The Second Xiangya Hospital of Central South University, Changsha, China  
E-mail: wanchun.wang@csu.edu.cn

Received: March 11, 2024; Revised: August 20, 2024;

Accepted: October 10, 2024

DOI: <https://doi.org/10.29271/jcpsp.2024.11.1831>

However, despite the potential of PANoptosis-related genes as prognostic markers and therapeutic targets in osteosarcoma, comprehensive models incorporating these genes are scarce. There is a critical gap in the literature regarding the systematic evaluation and validation of PANoptosis-related genes for predicting the prognosis of osteosarcoma patients. This study aimed to construct and validate a novel prognostic tool for osteosarcoma and highlight potential therapeutic targets based on PANoptosis-related genes using the LASSO-Cox regression.

## METHODOLOGY

Transcriptomic data were extracted from the GEO database (GSE16088), which included samples from 6 normal individuals and 16 patients with osteosarcoma. This dataset served as the foundation for the investigation into the genetic alterations affecting PANoptosis-related genes within osteosarcoma.

For the training cohort, RNA-sequencing data alongside clinical details from 85 osteosarcoma patients were retrieved from the TARGET database.<sup>13</sup> In contrast, the external validation cohort comprised RNA-sequencing data and corresponding clinical details for 53 osteosarcoma patients, sourced from the GEO database (GSE21257). Furthermore, the authors identified a set of 277 PANoptosis-related genes from an existing study,<sup>14</sup> contributing to this study.

The GSE16088 dataset was leveraged to perform a comparative analysis on the expression levels of PANoptosis-related genes between osteosarcoma samples and normal tissue. The *Limma* R package was used to identify PANoptosis-related DEGs.<sup>15</sup> The criteria for selection included genes exhibiting a  $|\log_{2}FC| > 0.585$  and  $FDR < 0.05$ . To identify differentially expressed PANoptosis-related genes with prognostic value, univariate Cox-regression analysis targeting overall survival (OS) was utilised.

To construct a prognostic model, TARGET-OS datasets were chosen as a training cohort, and PANoptosis-associated DEGs were integrated into a LASSO Cox-regression framework via the *Glmnet* R package.<sup>16</sup> Subsequently, genes identified through LASSO regression were further analysed using multivariate Cox-regression with the *survival* package,<sup>17</sup> aiming to develop a model capable of predicting patient outcomes. The risk score for each subject was computed based on the formula:

Risk score =  $\sum (\text{expression}(\text{Gene}_n) \times \text{coefficient}(\text{Gene}_n))$   
(expression (Gene<sub>n</sub>) denotes the expression level of a specific gene, and coefficient (Gene<sub>n</sub>) refers to its corresponding coefficient).

Based on the median risk score, patients were categorised into either low- or high-risk groups.

For external validation, the same prognostic model divided osteosarcoma patients from the GSE21257 dataset into comparable low- and high-risk categories, employing the identical median risk score criterion.

The independent predictive value of the signature was assessed using multivariate Cox-regression models. To evaluate the prognostic precision of the risk score across various datasets, Kaplan-Meier survival curves were utilised to assess the efficacy of the model in distinguishing between patient subtypes. The time-dependent receiver operating characteristic (ROC) curve and the incident / dynamic (I/D) area under the curve (AUC) metrics were employed, utilising the *time ROC* and *Riskset ROC* R packages, respectively.<sup>17,18</sup>

To ascertain the independent prognostic relevance of the risk score and assorted clinical parameters, both univariate and multivariate Cox-regression analyses were conducted. Factors exhibiting significance ( $p < 0.05$ ) in both analyses were identified as independent prognostic indicators and were subsequently incorporated into the development of a nomogram. The construction of this nomogram, aimed at predicting overall survival (OS), utilised the *survival* and *rms* R packages. The nomogram's predictive accuracy was quantified using the Concordance index (C-index) which varies between 0.5 and 1.0. A C-index approaching 1.0 denotes higher precision in the nomogram's predictive ability. The nomogram's performance was further assessed through Calibration curves for 1-year, 3-year, and 5-year OS predictions, comparing predicted outcomes with observed results. Ideally, a Calibration curve aligns closely with the 45-degree line, indicating accurate prediction.

The tumour immune microenvironment (TIME) characteristics across various molecular subtypes or PANscore categories were examined using the CIBERSORT algorithm. This involved assessing the infiltration of 22 immune cell types across all patient samples. Samples yielding  $p < 0.05$  were deemed accurately evaluated for immune cell infiltration and were selected for further analysis.

Furthermore, single nucleotide variation (SNV) and copy number variation (CNV) data from the TARGET-OS datasets were accessed. The mutational landscape was depicted using the waterfall function in the *maftools* R package, and Gistic 2.0 was utilised for CNV analysis.<sup>19</sup>

## RESULTS

A comparative analysis of the PANoptosis-related gene expression between osteosarcoma samples and normal tissues, using the GSE16088 dataset, revealed significant differential expression. Employing the *Limma* R package, numerous PANoptosis-related differentially expressed genes (DEGs) meeting a stringent criteria of  $|\log_{2}FC| > 0.585$  and  $FDR < 0.05$  were identified. These genes showed profound alterations in the osteosarcoma transcriptome, highlighting the potential mechanistic involvement of PANoptosis in tumorigenesis (Figure 1A), while their correlation coefficients were represented in Figure 1B.

Utilising the TARGET-OS dataset, a univariate Cox regression analysis of 277 PANoptosis-related genes identified 9 genes significantly associated with the survival of osteosarcoma patients (Figure 1C).

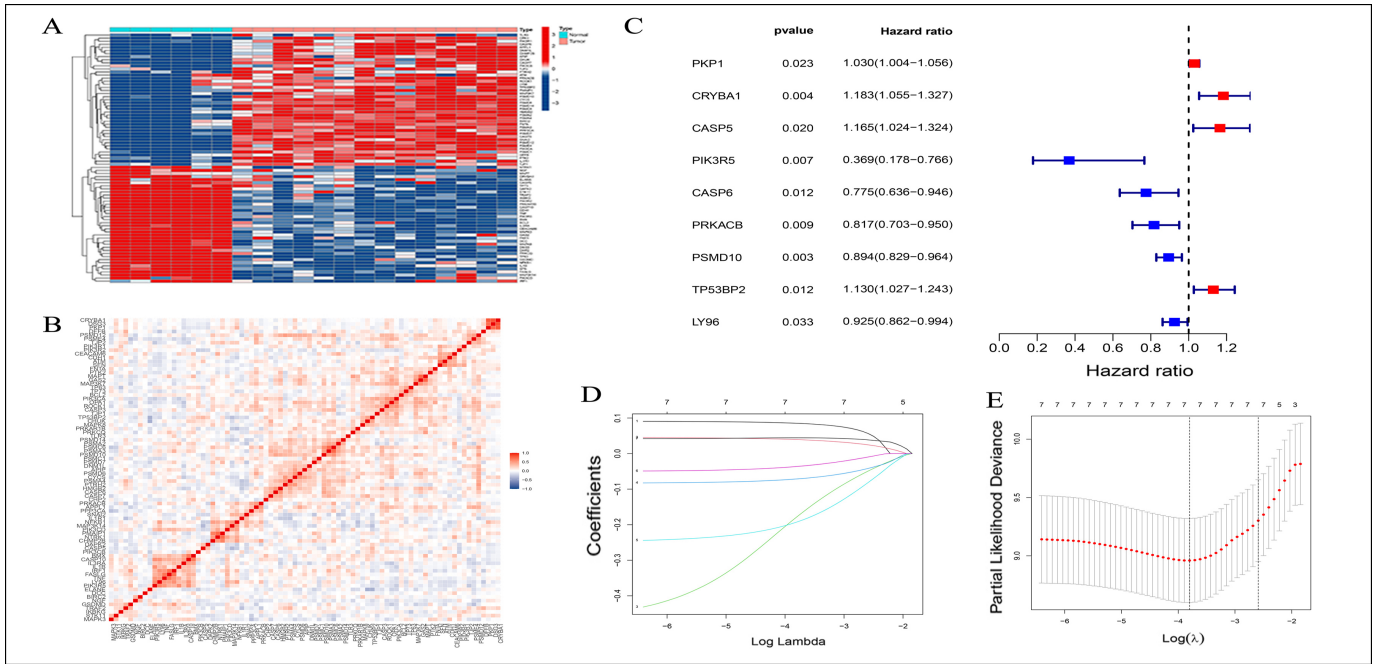


**Figure 1: Analysis of differentially expressed PANoptosis-related genes and development of the prognostic model. (A)** Heatmap of PANoptosis-related genes in the GSE16088 cohorts. **(B)** The correlation coefficient among the PANoptosis-related genes. **(C)** Forest plot of 9 PANoptosis-related genes significantly correlated with prognostic factors. **(D, E)** LASSO Cox-regression analysis was conducted on nine candidate PANoptosis-related genes to evaluate their prognostic significance, with the determination of the optimal penalty parameter for LASSO regression.

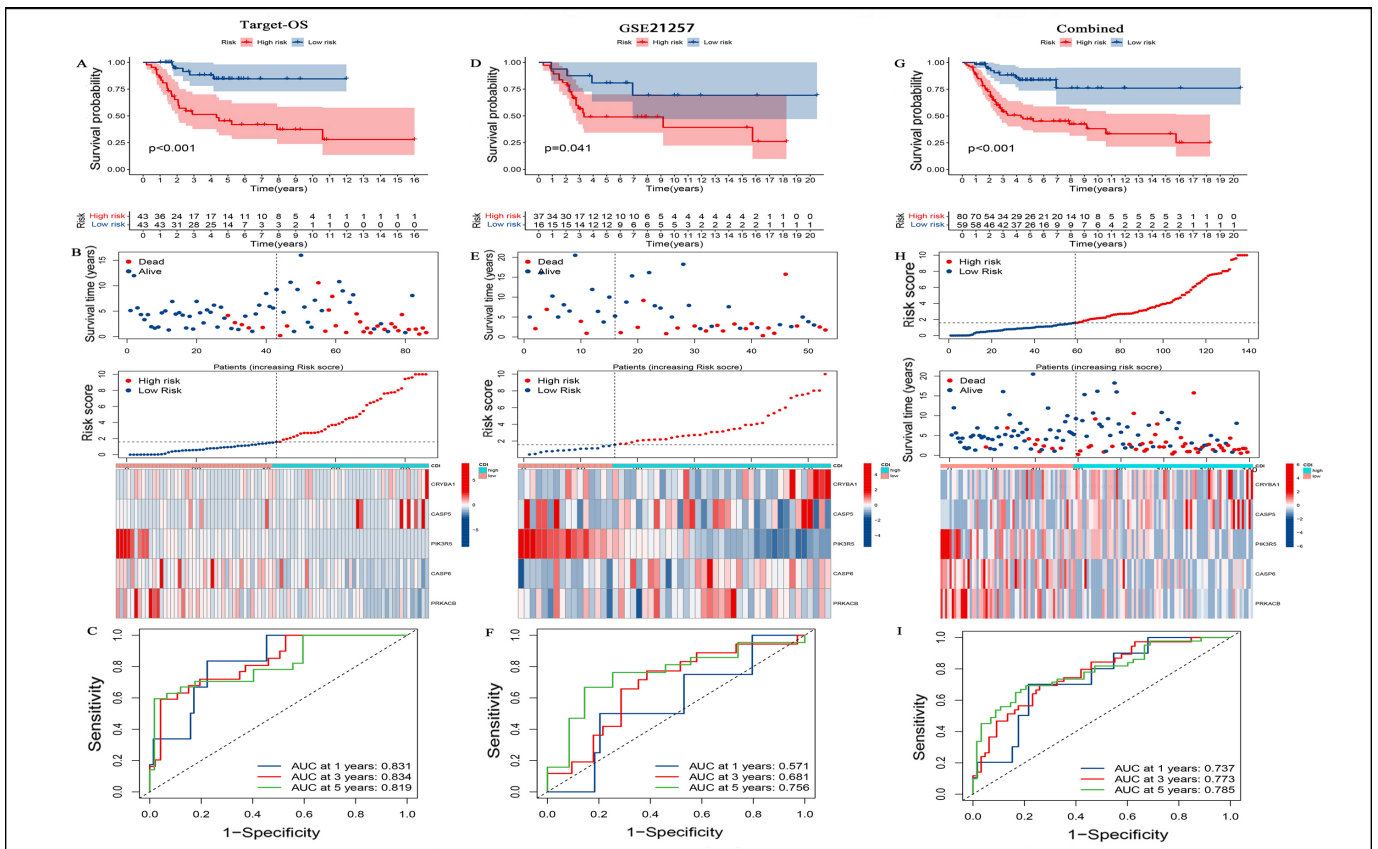


**Figure 2: Validation of the prognostic model. (A-C)** The Kaplan-Meier survival curves, survival status, risk heatmap, and ROC curve of patients in the TARGET-OS cohort. **(D-F)** The Kaplan-Meier survival curves, survival status, risk heatmap and ROC curve of patients in the GSE21257 cohort. **(G-I)** The Kaplan-Meier survival curves, survival status, risk heatmap, and ROC curve of all the patients from the TARGET-OS and GSE21257 datasets.

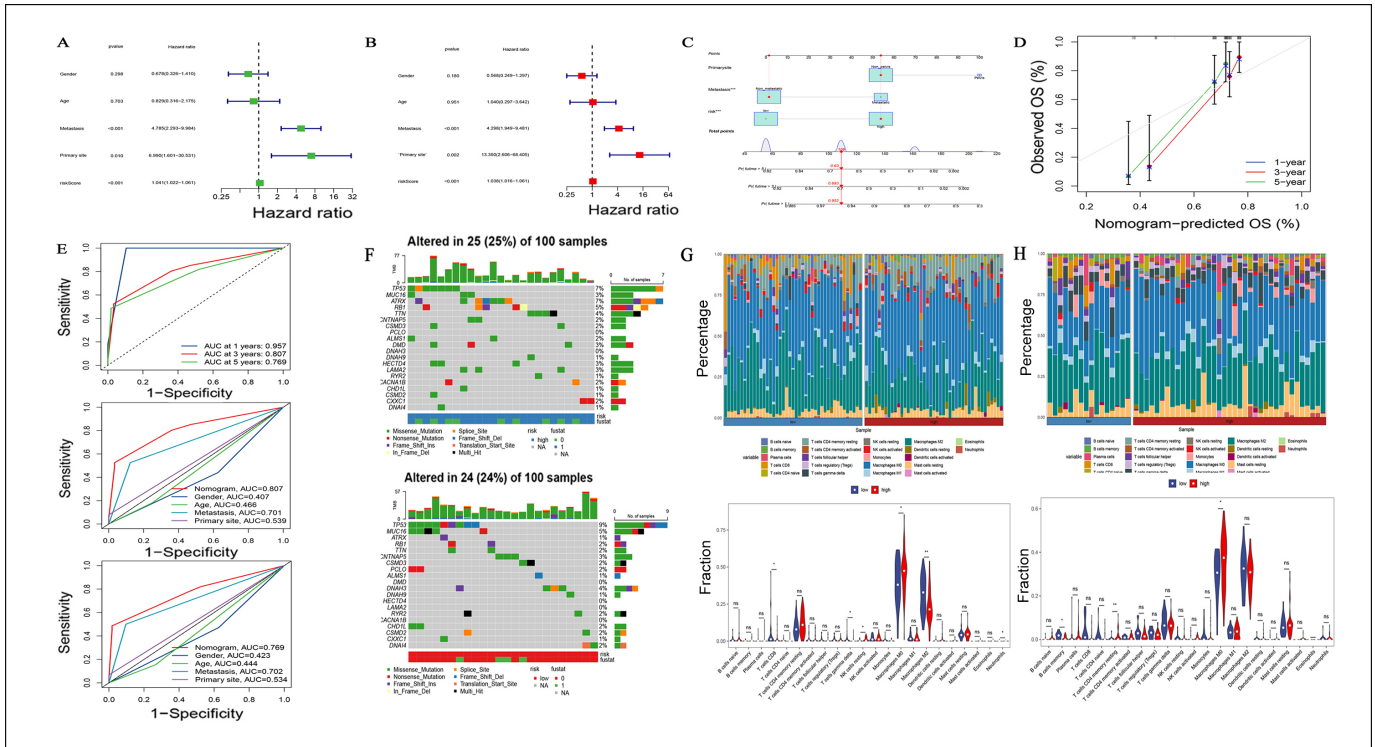


**Figure 3: Exploring the clinical utility of the prognostic model through nomogram development. (A) Analysis of risk scores through univariate and (B) Multivariate Cox-regression, incorporating variables such as gender, age, stage of metastasis, and primary tumour location. (C) Creation of a nomogram derived from multivariate Cox-regression analysis, aimed at predicting clinical outcomes within the TARGET-OS patient groups. (D) Calibration plots for the nomogram, designed to forecast overall survival (OS) at the 1-year, 3-year, and 5-year benchmarks within the TARGET-OS populations. (E) Assessment and comparison of the predictive performance of the risk score against other established models, using time-dependent ROC analysis to ascertain predictive accuracy over 1, 3, and 5 years among the TARGET-OS cohorts. (F) Illustration of the 20 most frequently mutated genes within the low-risk and high-risk groups. (G) Analysis of immune cell proportions and abundance across varying risk groups within the TARGET-OS population. (H) Analysis of immune cell proportions and abundance across varying risk groups within the GSE21257 cohort.**

To enhance the precision and simplify the predictive signature, LASSO regression and cox-stepwise regression analyses were employed to develop a prognostic model (Figure 1D and E), narrowing down the predictors to five essential genes: *CRYBA1*, *CASP5*, *PIK3R5*, *CASP6*, and *PRKACB*. The final prognostic model was established as follows:

$$\text{Risk score} = \text{CRYBA1} \times 0.0950938250121901 + \text{CASP5} \times 0.0613896146052882 - \text{PIK3R5} \times 0.51181272058199 - \text{CASP6} \times 0.103080159347395 - \text{PRKACB} \times 0.261801175025256.$$

The prognostic model's effectiveness was validated through Kaplan-Meier survival curve analysis in both the TARGET-OS and GSE21257 datasets. In the training set, the high-risk group as determined by the median risk score demonstrated significantly poorer survival than the low-risk group ( $p < 0.001$ , Figure 2A and 2B). This distinction was consistently observed in the validation set, reinforcing the model's predictive capability across the independent cohorts (Figure 2D and E) as well as the pooled dataset of TARGET-OS and GSE21257 (Figure 2G and H). Further analysis revealed that the prognostic risk score model had strong predictive capability for 1-year, 3-year, and 5-year patient survival rates, demonstrating excellent specificity

and sensitivity in predicting survival outcomes (Figure 2C and F, and 3).

To evaluate the independent prognostic ability of the PANoptosis-related genes risk signature, both univariate and multivariate Cox-regression analyses were conducted, incorporating risk scores and various patient clinical characteristics. A univariate Cox-regression analysis (Figure 3A) identified metastasis stage and risk scores as significant independent prognostic factors ( $p < 0.001$ ). Subsequent multivariate analysis (Figure 3B) further delineated that among these, metastasis stage and risk scores consistently emerged as robust independent prognostic indicators ( $p < 0.001$ ). Leveraging the TARGET-OS dataset, a predictive nomogram (Figure 3C) integrating risk scores with clinical parameters was crafted, aiming to enhance the prognostication for patients. Combined with the calibration plots (Figure 3D), it was observed that the predicted OS was consistent with the actual observations. The nomogram's efficacy was underscored through the ROC curve analysis (Figure 3E), revealing its superior predictive performance relative to the traditional clinical indicators. This superiority was further evidenced by the ROC curves for three- and five-year survival predictions (Figure 3E), showcasing the nomogram's heightened predictive capability for patient outcomes.

This study explored the association between the PANoptosis-related genes risk score, tumour mutational landscapes, and immune infiltration profiles. The analysis revealed a distinct somatic mutation landscape across PANoptosis-related genes (PAN\_DEGs) subgroups, highlighting the top 20 mutated genes including *TP53*, *MUC16*, and *ATRX*, among others (Figure 3F). Notably, *TP53* emerged as the most frequently mutated gene, with a higher mutation rate observed in the low-risk score subgroup compared to the high-risk score group. Further, an immunological landscape analysis, conducted within both TARGET-OS (Figure 3G) and GSE21257 (Figure 3H) datasets, demonstrated significant variations in the distribution of 22 immune cell types across the subgroups. This comprehensive analysis underscores the intricate interplay between the PANoptosis-related genes risk score, tumour mutation burden, and immune cell infiltration, offering novel insights into the potential mechanisms driving these associations.

## DISCUSSION

The findings of this study underscore the critical role of PANoptosis-related genes in the prognosis of osteosarcoma, highlighting a novel prognostic model that effectively predicts patient outcomes.

Osteosarcoma is linked to the dysregulation of cell death mechanisms and inflammatory responses. Genes associated with PANoptosis have been cited in the context of various other tumours.<sup>20</sup> Members of the *Caspase* family are implicated in tumour progression.<sup>21</sup> The identified genes within the model may serve as potential targets for the novel therapeutic strategies, aiming to modulate the pathways of programmed cell death to improve patient outcomes.

This study contributes to this growing body of knowledge by exploring the correlation between tumour immune infiltration levels, genetic changes, and risk stratification in cancer patients.<sup>22</sup>

Research has demonstrated that the tumour microenvironment, characterised by the immune cell infiltration, plays a pivotal role in cancer progression and therapeutic response.<sup>23</sup> Tumour mutational burden (TMB) significantly correlates with immune scores and tumour purity, indicating that high TMB levels are associated with altered immune infiltration. Differences in the proportion of various types of immune cells, such as CD8<sup>+</sup> T cells and macrophages, were linked to survival outcomes.<sup>24</sup> A study on prostate cancer reinforced the connection between genetic variations, immune cell infiltration, and patient risk stratification. It was found that certain somatic mutations were more prevalent in the high-risk groups, which also correlated with differences in tumour-infiltrating immune cells.<sup>25</sup>

This research aligns with these findings, suggesting that the interplay between genetic variations and the level of tumour immune infiltration can significantly impact the prognosis of cancer patients. This underscores the need for further investigation into the mechanisms driving these associations and their implications for cancer treatment and patient care.

To enhance the generalisability and clinical applicability of this prognostic model, future studies should focus on validating the model across larger, more diverse populations, and in various clinical settings. The lack of prospective validation is a limitation of this study, as real-time patient data would provide a more accurate assessment of the model's performance. The authors recommend that future research should include prospective studies to confirm the utility of PANoptosis-related gene signatures in osteosarcoma prognosis and to explore their potential in guiding therapeutic strategies.

The Kaplan-Meier curves demonstrate a clear separation between the high-risk and low-risk patient groups, indicating the model's ability to stratify the patients based on survival probability.

Furthermore, the time-dependent ROC curves underline the predictive precision of the risk score, with AUC values exceeding 0.70 across different time points (1-year, 3-year, and 5-year survival), reinforcing the model's robustness. These graphical insights confirm that the proposed model not only offers a novel tool for osteosarcoma prognostication but also holds potential for guiding therapeutic decisions by identifying high-risk patients who may benefit from more aggressive treatment strategies.

The integration of PANoptosis-related gene analysis in osteosarcoma prognostication, supported by rigorous graphical validation, highlights the clinical utility of this model. Future research should focus on prospective validation in diverse populations to further solidify the model's applicability and explore its potential in guiding personalised treatment approaches.

## CONCLUSION

This study elucidates the prognostic significance of PANoptosis-related genes in osteosarcoma by presenting a validated model that effectively predicts patient outcomes. The graphical representations, including Kaplan-meier survival curves and ROC curves, provide strong visual evidence of the model's discriminatory power.

### ETHICAL APPROVAL:

The study was initiated after obtaining ethical approval from the Ethical Review Committee of the Second Xiangya Hospital, Hunan, Xiangya, China (Approval No.: LYEC2024-0093).

**PATIENTS' CONSENT:**

This study did not involve direct patient data; hence, no informed consent was required.

**COMPETING INTEREST:**

The authors declared that the research was conducted in the absence of any commercial or financial relationships that could be construed as a potential conflict of interest.

**AUTHORS' CONTRIBUTION:**

XP: Conducted the investigation and drafted the manuscript.

XP, WW: Conceived and designed the study, critically revised the manuscript for the important intellectual content.

Both authors approved the final version of the manuscript to be published.

**REFERENCES**

- Beird HC, Bielack SS, Flanagan AM, Gill J, Heymann D, Janeway KA, et al. Osteosarcoma. *Nat Rev Dis Primers* 2022; **8(1)**:77. doi: 10.1038/s41572-022-00409-y.
- Sung H, Ferlay J, Siegel RL, Laversanne M, Soerjomataram I, Jemal A, et al. Global cancer statistics 2020: GLOBOCAN estimates of incidence and mortality worldwide for 36 cancers in 185 countries. *CA Cancer J Clin* 2021; **71(3)**:209-49. doi: 10.3322/caac.21660.
- Sajadi KR, Heck RK, Neel MD, Rao BN, Daw N, Rodriguez-Galindo C, et al. The incidence and prognosis of osteosarcoma skip metastases. *Clin Orthop Relat Res* 2004; **(426)**:92-6. doi: 10.1097/01.blo.0000141493.52166.69.
- Huang X, Zhao J, Bai J, Shen H, Zhang B, Deng L, et al. Risk and clinicopathological features of osteosarcoma metastasis to the lung: A population-based study. *J Bone Oncol* 2019; **16**:100230. doi:10.1016/j.jbo.2019.100230.
- Isakoff MS, Bielack SS, Meltzer P, Gorlick R. Osteosarcoma: Current treatment and a collaborative pathway to success. *J Clin Oncol* 2015; **33(27)**:3029-35. doi: 10.1200/jco.2014.59.4895.
- Pandian N, Kanneganti TD. PANoptosis: A unique innate immune inflammatory cell death modality. *J Immunol* 2022; **209(9)**:1625-33. doi: 10.4049/jimmunol.2200508.
- Christgen S, Tweedell RE, Kanneganti TD. Programming inflammatory cell death for therapy. *Pharmacol Ther* 2022; **232**:108010. doi: 10.1016/j.pharmthera.2021.108010.
- Pan B, Zheng B, Xing C, Liu J. Non-canonical programmed cell death in colon cancer. *Cancers (Basel)* 2022; **14(14)**:3309. doi: 10.3390/cancers14143309.
- Zhang B, Huang B, Zhang X, Li S, Zhu J, Chen X, et al. PANoptosis-related molecular subtype and prognostic model associated with the immune microenvironment and individualized therapy in pancreatic cancer. *Front Oncol* 2023; **13**:1217654. doi: 10.3389/fonc.2023.1217654.
- Ocansey DKW, Qian F, Cai P, Ocansey S, Amoah S, Qian Y, et al. Current evidence and therapeutic implication of PANoptosis in cancer. *Theranostics* 2024; **14(2)**:640-61. doi: 10.7150/thno.91814.
- Brion R, Gantier M, Biteau K, Taurelle J, Brounais-Le Royer B, Verrecchia F, et al. TRAIL-based therapies efficacy in pediatric bone tumors models is modulated by trail non-apoptotic pathway activation via ripk1 recruitment. *Cancers (Basel)* 2022; **14(22)**:5627. doi: 10.3390/cancers14225627.
- Ning X, Shang XW, Zhuang Y, Liu M, Yang H, Zhang H, et al. Correlation between TRAIL and caspase-8 expression and their relationship with cell proliferation and apoptosis in human osteosarcoma. *Genet Mol Res* 2016; **15(4)**. doi: 10.4238/gmr15048876.
- Hutter C, Zenklusen JC. The cancer genome atlas: creating lasting value beyond its data. *Cell* 2018; **173(2)**:283-5. doi: 10.1016/j.cell.2018.03.042.
- Yang Z, Kao X, Huang N, Yuan K, Chen J, He M. Identification and analysis of panoptosis-related genes in sepsis-induced lung injury by bioinformatics and experimental verification. *J Inflamm Res* 2024; **17**:1941-56. doi: 10.2147/jir.S452608.
- Ritchie ME, Phipson B, Wu D, Hu Y, Law CW, Shi W, et al. Limma powers differential expression analyses for RNA-sequencing and microarray studies. *Nucleic Acids Res* 2015; **43(7)**:e47. doi: 10.1093/nar/gkv007.
- Friedman J, Hastie T, Tibshirani R. Regularization paths for generalized linear models via coordinate descent. *J Stat Softw* 2010; **33(1)**:1-22.
- Le-Rademacher JG, Therneau TM, Ou FS. The utility of multistate models: A flexible framework for time to event data. *Curr Epidemiol Rep* 2022; **9(3)**:183-9. doi: 10.1007/s40471-022-00291-y.
- Therneau TM, Grambsch PM. Modeling Survival Data: Extending the Cox Model. New York: Springer; 2000.
- Mayakonda A, Lin DC, Assenov Y, Plass C, Koeffler HP. Maftools: efficient and comprehensive analysis of somatic variants in cancer. *Genome Res* 2018; **28(11)**:1747-56. doi: 10.1101/gr.239244.118.
- Wang M, Yu F, Zhang Y, Li P. Programmed cell death in tumor immunity: mechanistic insights and clinical implications. *Front Immunol* 2023; **14**:1309635. doi: 10.3389/fimmu.2023.1309635.
- Jiang M, Qi L, Li L, Wu Y, Song D, Li Y. Caspase-8: A key protein of cross-talk signal way in "PANoptosis" in cancer. *Int J Cancer* 2021; **149(7)**:1408-20. doi:10.1002/ijc.33698.
- Liu J, Hong M, Li Y, Chen D, Wu Y, Hu Y. Programmed cell death tunes tumor immunity. *Front Immunol* 2022; **13**:847345. doi:10.3389/fimmu.2022.847345.
- Zhao H, Yin X, Wang L, Liu K, Liu W, Bo L, et al. Identifying tumour microenvironment-related signature that correlates with prognosis and immunotherapy response in breast cancer. *Sci Data* 2023; **10(1)**:119. doi: 10.1038/s41597-023-02032-2.

24. Wang H, Liu J, Yang J, Wang Z, Zhang Z, Peng J, *et al.* A novel tumor mutational burden-based risk model predicts prognosis and correlates with immune infiltration in ovarian cancer. *Front Immunol* 2022; **13**:943389. doi: 10.3389/fimmu.2022.943389.
25. Xie LY, Huang HY, Hao YL, Yu M, Zhang W, Wei E, *et al.* Development and validation of a tumor immune cell infiltration-related gene signature for recurrence prediction by weighted gene co-expression network analysis in prostate cancer. *Front Genet* 2023; **14**:1067172. doi: 10.3389/fgene.2023.1067172.

